

Many Electron Correlations in Stage-1 Graphene Intercalation Compounds

Sidharth Acharya¹, Raman Sharma²

^{1,2}Department of Physics Himachal Pradesh University, Shimla
Summer Hill, Shimla, INDIA

ABSTRACT

Many electron correlations in stage-1 graphene intercalation compounds GICs are studied in generalized random-phase-approximation. With this approximation, we are able to study short range exchange and correlation effects in GICs. These exchange correlations leads to BCS superconducting states in which one electron correlates with another via its correlation hole to form a stable pair of electrons known as Cooper pair. Cooper pair energies are calculated as the excitations in $S(q,\omega)$ following a method similar to exciton energy calculations. Short range effects governing local field correction $G(q,\omega)$ are studied valid for all wavevectors and frequencies. We have found a reasonable agreement between our results and the earlier theoretical results.

Keywords: *GICs, dielectric function, energy loss function, local field correction factor*

1. INTRODUCTION

There have been made many efforts to understand the many electron correlations within a short range $\mathbf{r}=0$ known as short-range correlations in uniform electron gas^{1,2}. Basic assumption is that exchange-correlation effects leads to a local depletion in the density around each electron. The effective field acting on an electron differs from the macroscopic mean field which led to the concept of local field correction. Here we have studied short-range correlations in stage-1 graphene intercalation compounds (GICs) which is considered as layered massless-Dirac Fermion gas (MDF) in generalized-random-phase-approximation^{3,4}.

We use many electron correlation function to study exchange-correlation effects in GICs². This describes interaction between the first particle and all surrounding particles in presence of the second particle. This can be considered as an electron occupying a state $\mathbf{k}\uparrow$ interacts with second electron occupying a state $-\mathbf{k}\downarrow$ attractively via its correlation hole to which it is bound (known as an exciton) at $\mathbf{r}=0$. This forms a stable cooper pair in the BCS superconducting state which is lowered in energy than normal state by an amount the binding energy of Cooper pair⁵. An exciton can therefore form Cooper pairs with all surrounding ones.

We consider GICs as type-II superlattices^{3,6} with graphene-intercalant heterojunction consisting of a spatial separation and confinement of electrons and holes with a typical carrier density $\sim 10^{12} \text{ cm}^{-3}$. Such a high carrier density is achieved by a charge transfer across graphene-intercalant heterojunction due to unusual line up of bulk energy bands. Electrons released by donors drop into the potential wells of graphene host. The one dimensional potential well acts as a superconducting channel for Cooper pairs which quantize the electronic motion along superlattice direction. With increase in the carrier density graphene conduction band split into a series of sub-bands and the band degeneracy around Fermi energy is removed. There exists an energy gap which increases with increase in the degree of charge transfer. Each sub-band acting as a superconducting channel represents free-effective-mass type electronic motion in the plane perpendicular to the superlattice direction. At low temperatures $T \rightarrow 0$ only the lowest sub-band is occupied and the superlattice can be considered as Bose-Einstein condensate (BEC) in which paired electrons exhibit bosonic characteristics.

In this paper we have developed the dielectric function for GICs in generalized-random-phase-approximation^{4,2}. Numerical calculations are made to explore the superconducting energy states which gives Cooper pair energies and to study short range local field correction.

2. GENERALIZED-RANDOM-PHASE-APPROXIMATION

2.1 Dielectric Function

We consider GICs as type two superlattices comprised of massless Dirac fermion gas MDF³. Excitons so formed are free particles, mutually interacting by Coulomb potential e^2/r . At $T \rightarrow 0 \text{ K}$ graphene intercalant sublattices can be treated individually (by neglecting c-axis couplings). This gives density of host $D(E_F) = g_v g_s |2E_F| / \sqrt{3} \gamma_0^2$, which vanishes as $E_F \rightarrow 0$ at $T \rightarrow 0 \text{ K}$. This is an universal feature of all low dimensional materials.

This is also a characteristics feature of a superconductor where energy gap is centered at the Fermi level⁵. Thus at absolute zero no current can flow until the applied voltage is $E_g/2e = \Delta/e$, where E_g is the energy gap in the superconducting state. The energy gap corresponds to the break-up of a pair of electrons in the superconducting state with the formation of two electrons, or an electron and a hole in the normal state. The current starts when $eV = \Delta$.

In generalized-random-phase-approximation^{2,4} dielectric function of GICs can be obtained by solving equation of motion for many particle distribution function

$$\epsilon^{\text{GRPA}}(\mathbf{q}, \omega) = \epsilon_i(\mathbf{q}, \omega) + \epsilon_s(\mathbf{q}, \omega) + \epsilon_{i+s}(\mathbf{q}, \omega), \quad (1)$$

which is the sum of dielectric function due to induced potential, dielectric function due to screening potential, and dielectric function due to equal time correlation potential between two particles in presence of all surrounding ones. We have

$$\begin{aligned} \varepsilon_i(\mathbf{q}, \omega) &= 1 - v(\mathbf{q})S(\mathbf{q}, k_z) \frac{g_v g_s}{S} \sum_{\mathbf{k}\mathbf{k}'ss'} \frac{\bar{f}_{\mathbf{k}-\mathbf{q},\mathbf{k}'ss'}^2 - \bar{f}_{\mathbf{k}+\mathbf{q},\mathbf{k}'ss'}^2}{E_{s'\mathbf{k}} - E_{s\mathbf{k}+\mathbf{q}} + \omega} \times |c_{s\mathbf{k}+\mathbf{q}}^\dagger, c_{s'\mathbf{k}}|^2 \\ + \varepsilon_s(\mathbf{q}, \omega) &= 1 - v(\mathbf{q})S(\mathbf{q}, k_z)\chi(\mathbf{q}, \omega), \\ + \varepsilon_{i+s}(\mathbf{q}, \omega) &= 1 - v(\mathbf{q})S(\mathbf{q}, k_z) \frac{g_v g_s}{S} \sum_{\mathbf{k}\mathbf{k}'ss'} \frac{\bar{f}_{\mathbf{k}-\mathbf{q},\mathbf{k}',k''ss'}^3 - \bar{f}_{\mathbf{k}+\mathbf{q},\mathbf{k}',k''ss'}^3}{E_{s'\mathbf{k}} - E_{s\mathbf{k}+\mathbf{q}} + \omega} \end{aligned} \quad (2)$$

where $v(\mathbf{q})=2\pi e^2/\varepsilon_0 q$ is the Fourier transform of the two-dimensional Coulomb potential, $S(\mathbf{q}, k_z)=2/qI_c$ for $k_z=0$ and $qI_c/2$ for $k_z=\pi/I_c$ is the structure factor where k_z is confined to the first Brillouin zone. $ss'=\pm 1$ are the band indices for conduction and valance bands respectively. $g_v g_s=2$ are the spin and valley degeneracies and S is the sample area. Polarization function $\chi(\mathbf{q}, \omega)$ for large \mathbf{q} is given by

$$\chi(\mathbf{q}, \omega) = \chi^0(\mathbf{q}, \omega)[1 + v(\mathbf{q})\{1 - G(\mathbf{q}, \omega)\}]\chi^0(\mathbf{q}, \omega), \quad (3)$$

which arise as a constant of proportionality and is independent of the number of layers in GIC's. Free particle polarizability is given by

$$\chi^0(\mathbf{q}, \omega) = \frac{1}{S} \sum_{\mathbf{k}ss'} \frac{f_{s'\mathbf{k}}^0 - f_{s\mathbf{k}+\mathbf{q}}^0}{E_{s'\mathbf{k}} - E_{s\mathbf{k}+\mathbf{q}} + \omega} |c_{s\mathbf{k}+\mathbf{q}}^\dagger c_{s'\mathbf{k}}|^2, \quad (4)$$

which describes the effect of polarization of free excitons such that $f_{s'\mathbf{k}=1,0}^0$ for conduction and valance bands respectively. $f_{\mathbf{k}\mathbf{k}'ss'}^2$ and $f_{\mathbf{k}\mathbf{k}'k''ss'}^3$ are the two and three particle distribution functions. $|c_{s\mathbf{k}+\mathbf{q}}^\dagger c_{s'\mathbf{k}}|^2 = [1 + ss'\cos(\theta_{\mathbf{k}} - \theta_{\mathbf{k}+\mathbf{q}})]/2$ are the Coulomb matrix elements. It is a measure of transition probability in a given direction. As $\uparrow\mathbf{k} \rightarrow -\downarrow\mathbf{k}$, the Coulomb matrix elements vanishes and indicates that the two electrons cannot have the same quantum state in accordance with Pauli's exclusion principle. The polarization function vanishes and exciton is unstable with respect to radiative recombination in which the electron drops into the hole in the valance band and there is an absence of backscattering in GICs.

2.2 BCS Superconducting States

The response to an external perturbation which varies rapidly in space is determined by the free particle behavior. This is because a free particle travels a certain distance before it is affected by the presence of other particles. In fact when two electrons form a Cooper pair their mutual interaction dominates over the interactions with the surrounding particles. It is then sufficient to solve two-

body problem included in $\epsilon_s(\mathbf{q}, \omega)$. The superconducting states can be obtained as transition peaks in $S(\mathbf{q}, \omega)^{3,7}$

$$S(\mathbf{q}, \omega) = -\frac{1}{nv(\mathbf{q})S(\mathbf{q}, k_z)} \text{Im} \left[\frac{1}{\epsilon_s(\mathbf{q}, \omega)} \right] \quad (5)$$

In fig. 1 (a) we have a plot of $\text{Im}[-1/\epsilon_s(\mathbf{q}, \omega)]$ versus ω at selected \mathbf{q} . This gives superconducting states in the two coupling limits determined by structure factor $S(\mathbf{q}, k_z)$. The minimum threshold for the super current to flow is $\Delta \sim 0.2\text{eV}$ with forbidden intraband transitions $v \rightarrow v$ or $c \rightarrow c$ because of vanishing polarization function at $\mathbf{q} = 2\mathbf{k}_F$. This requires a removal of band degeneracies around the Fermi point so that all interband transitions $v \rightarrow c$ separated by an energy gap are allowed. In fact, charge transfer in GICs increases with the applied voltage and energy gap depends on the degree of charge transfer.

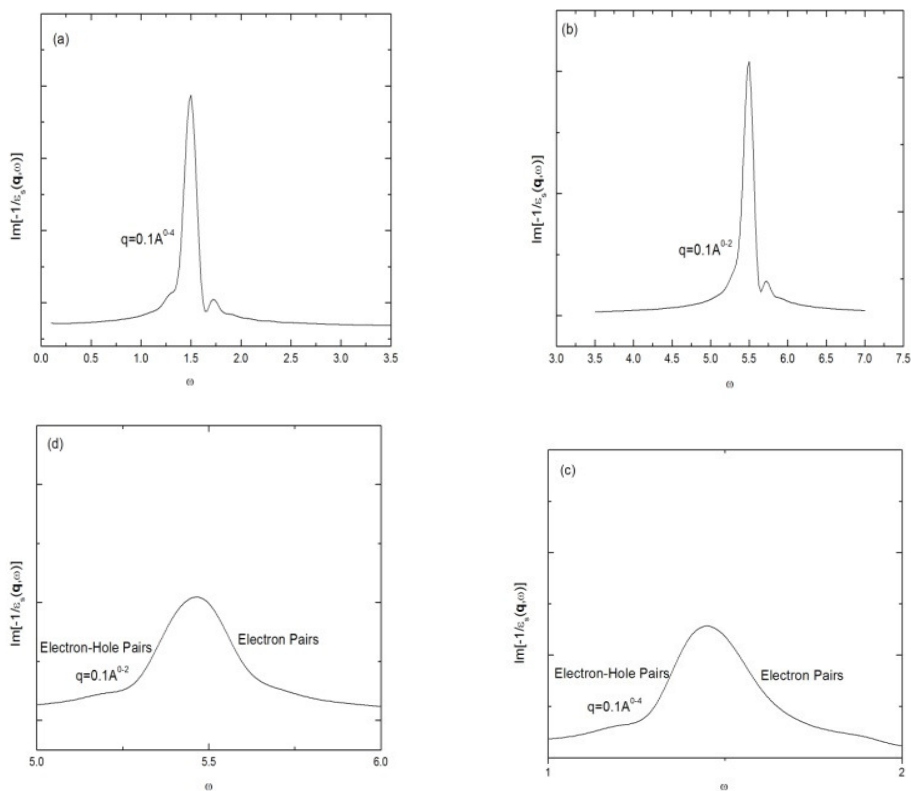


Figure. 1- (a) A plot of $\text{Im}[-1/\epsilon_s(\mathbf{q}, \omega)]$ versus ω representing BCS superconducting state at selected \mathbf{q} near the upper edge of the weak coupling limit. (b) A plot of $\text{Im}[-1/\epsilon_s(\mathbf{q}, \omega)]$ versus ω representing BCS superconducting state at selected \mathbf{q} in the strong coupling limit. (c) A plot of two-dimensional broadening obtained from curve (a). (d) A plot of two-dimensional broadening obtained from curve (b).

Near the upper edge of weak coupling $k_z=\pi/l_c$ we have found an interband transition at 1.5eV corresponding to the interband threshold of 1.47eV in C_6FeCl_3 . This difference in energies ~ 0.03 eV gives cooper pair energy. Compared with exciton energies cooper pair energy is negative. This is expected because a free exciton on acquisition of energy interacts with another one in the normal state to form a Cooper pair in the superconducting state. Energy released during this process is the binding energy of Cooper pair. Thus superconducting states at small energies are exceptionally stable at $T \rightarrow 0$, where MDF gas in GICs exhibits three-dimensional behavior with q^{-4} dependence. In fig. 1 (b) we have shown a superconducting energy state corresponding to the interband threshold of 5.47eV in C_6FeCl_3 in the limit of strong coupling $k_z=0$. We have found an interband transition at 5.5eV and the binding energy of the cooper pair is ~ -0.03 eV which is same as the weak coupling case. A large energy gap causes few free carriers to make interband transitions. At high energies these free carriers involves multiple collisions. Each collision causes a free exciton and a covalent bond is broken. The number of Cooper pairs formed however are small as compared to number of free electron-hole pairs formed in multiple collisions which results the Zener breakdown with further increase in energies. GICs are therefore superconducting within a certain (1.5eV to 5.5eV) range of applied field which is a characteristics of type-II superconductor. It should be noted that the interband threshold values for GICs varies from sample to sample. In fig. 1 (c) and 1 (d) we have shown a plot of two-dimensional broadenings obtained from superconducting states (a) and (b). Broadening here corresponds to electron-hole pairs in the normal state and free electron pairs in BCS superconducting state. This is a consequence of the layered structure of GICs.

The intrinsic length⁵ ξ_0 can be obtained in terms of modulated density distribution $\xi_0=1/q_0$, where

$$q_0 = \frac{2m^*E_g}{\hbar k_F} = \frac{E_g}{v_0} \quad (6)$$

This gives $\xi_0=500 \times 10^{-8}$ m with $E_g=1.47$ eV and $\xi_0=118 \times 10^{-8}$ m with $E_g=5.47$ eV, in the limits of weak and strong couplings respectively. Intrinsic length shows a decrease with increase in interband threshold. The superconducting electron concentration cannot change drastically at low energies and GICs are characterized by a stable superconducting state. The intrinsic coherence length can be compared with graphene bilayer $\sim 10^{-8}$ m measured from central Dirac point⁸. The penetration depth $\lambda_L = (m^*c^2/4\pi ne^2)^{1/2}$ assume a value $\sim 6.42 \times 10^{-3}$ cm. This gives $\kappa = \lambda_L/\xi_0=12$ and 54 at 1.47eV and 5.47eV respectively. This further indicates GICs are type-II superconductors for $\kappa > 1$ in the energy range of interest. At small incident energies and at $T \rightarrow 0$ only the lowest sub-band is filled and MDF gas forms the so called Bose-Einstein Condensate in which paired electrons (by s-wave pairing the simplest case considered) exhibit bosonic properties. With increase in charge

transfer a vortex state is formed in GICs which provides stable superconducting channels. Transition temperature for C_6FeCl_3 can be obtained in BCS theory $\Delta=1.76k_B T_c=0.48K-1.80K$ with $k_B=0.8625 \times 10^{-4}$ eV in the energy range of interest⁹.

3. LOCAL FIELD CORRECTION

If the external field varies rapidly in space and time the response of the system is determined by the motion of particles for short times as they travel certain distance before being affected by the other ones. In BCS state it requires that a spin up electron is at r if a spin down electron is at $r=0$. Of course, electrons are not fixed, and are usually moving rapidly. Even the electron at $r=0$ is not fixed, it is assumed that the reference point moves with the electron. Pair distribution function therefore averages for moving particles and in the Hartree-Fock approximation $g\uparrow\downarrow=g\downarrow\uparrow=1/2=g(0)$. In GICs the lowest energy state is at $T \rightarrow 0$, which is the state with some correlation between the motion of the electrons with anti-parallel spins. The basic process takes an electron from below to above the Fermi level. It leaves a vacancy in the Fermi sea which is the hole. If electron is going forward in time hole is going backward in time. Electron is bound to hole which is an exciton in normal state and excitons mutually interact to form Cooper pairs in superconducting state.

In Hartree-Fock approximation local field correction $G(\mathbf{q}, \omega)$ is obtained from many particle distribution function by solving two particle part²

$$G(\mathbf{q}, \omega) = \alpha(\mathbf{q}, \omega) \sum_{\mathbf{q}' s s'} \frac{(\mathbf{s} \cdot \mathbf{q}' \cdot \mathbf{q}')^2 v(\mathbf{q}')}{q^4 v(\mathbf{q})} [s(\mathbf{q}') - 1] \\ - \frac{1}{N} \sum_{\mathbf{q}' s s'} \left[\frac{\mathbf{s} \cdot (\mathbf{q}' + \mathbf{q})}{q^2} \right]^2 \frac{v(\mathbf{q} + \mathbf{q}')}{v(\mathbf{q})} [s(\mathbf{q}') - 1], \quad (7)$$

where

$$\alpha(\mathbf{q}, \omega) = \frac{1}{2} \left[\frac{\hbar\omega + \hbar^2 q^2 / 2m}{\hbar\omega - \hbar^2 q^2 / 2m} + \frac{\hbar\omega - \hbar^2 q^2 / 2m}{\hbar\omega + \hbar^2 q^2 / 2m} \right].$$

this result is valid for any arbitrary potential. The first term describes the motion of a Cooper pair in BCS superconducting state in which an electron correlates with another via its correlation hole. It contains a drastic frequency dependence. Second term is associated with a bound electron hole pair, i.e., exciton. It describes dynamics of the correlation hole. This term represents a proper local

field correction in MDF gas when compared with uniform electron gas. For large \mathbf{q} and at finite frequencies this gives

$$\lim_{q \rightarrow \infty} G(\mathbf{q}, \omega) = 1 - g(0) = \frac{1}{2}, \quad (8)$$

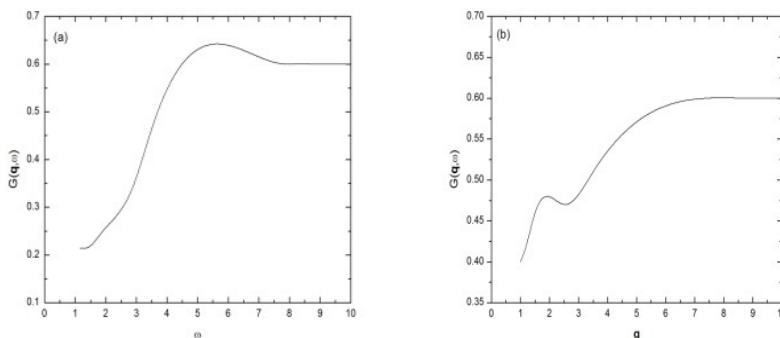


Figure. 2- (a) A plot of $G(\mathbf{q}, \omega)$ versus ω . (b) A plot of $G(\mathbf{q}, \omega)$ versus \mathbf{q} .

which has been referred to as an exact condition for local field correction^{1,10}. We have made a numerical calculation of $G(\mathbf{q}, \omega)$ given in eqn. (7) valid for all frequencies and wave vectors. Since the linear response theory employs the concepts of responses, excitations and relaxations the best way to evaluate the first term in eqn. (7) is in the relaxation regime after excitation pulse with absolute convergent values of $G(\mathbf{q}, \omega)$. This makes the two terms identical with different contributions to $G(\mathbf{q}, \omega)$ which are then added together. In fig. 2 (a) we have a plot of $G(\mathbf{q}, \omega)$ versus ω valid for all ω . $G(\mathbf{q}, \omega)$ is a dimensional quantity whereas ω is measured in eV. The convergent values of $G(\mathbf{q}, \omega)$ are obtained over a range of ω values which are averaged to obtain absolute convergent $G(\mathbf{q}, \omega)$. The curve near 5.5eV exhibits stable BCS superconducting states and the variation with ω is more sensitive at high energies. In fig. 2 (b) we have a plot of $G(\mathbf{q}, \omega)$ versus \mathbf{q} valid for all \mathbf{q} . Here, plotted values as expected show a smoothed curve except for BCS superconducting states which can be observed near 1.5eV. Thus, the variation with \mathbf{q} is more sensitive at low energies. This further shows less variations of $G(\mathbf{q}, \omega)$ with \mathbf{q} because in the Hartree-Fock approximation $g(0)=1/2$ only. The plotted values are in good agreement with those obtained by Goran Niklasson² for large \mathbf{q} and finite ω . Our plotted values follow

$$\frac{1}{4} < G(\mathbf{q}, \omega) < \frac{2}{3}, \quad (9)$$

and

$$\frac{2}{5} < G(\mathbf{q}, \omega) < \frac{2}{3}. \quad (10)$$

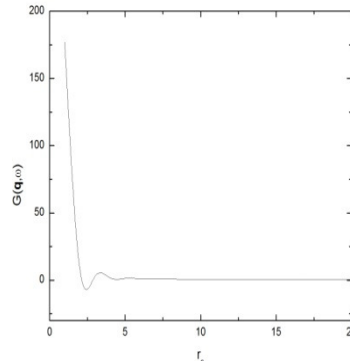


Fig. 3- A plot of $G(\mathbf{q}, \omega)$ versus r_s .

In fig. 3 we have a plot of $G(\mathbf{q}, \omega)$ versus r_s parameter. This shows the nature of potential between two interacting electrons via correlation hole forming a Cooper pair. As expected the curve shows an attractive interaction in the range of interest. This confirms the fact that Cooper pairs interact attractively and superconducting state is lower in energy than normal state. In fig. 4 (a) we have shown a plot of $\chi(\mathbf{q}, \omega)$ versus ω obtained by inserting $G(\mathbf{q}, \omega)$ values in dielectric function $\epsilon_s(\mathbf{q}, \omega)$.

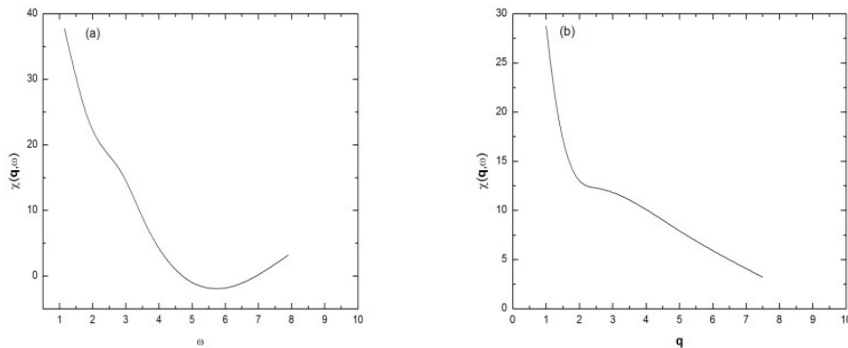


Figure. 4-(a) A plot of $\chi(\mathbf{q}, \omega)$ versus ω . (b) A plot of $\chi(\mathbf{q}, \omega)$ versus q .

As expected the variation shows stable superconducting states near low and high energies $\sim 1.5\text{eV}$ and 5.5eV . In fig. 4 (b) we have $\chi(\mathbf{q}, \omega)$ versus q curve which shows stable superconducting states near low energies.

3. CONCLUSION

We have used many electron correlation function to obtain dielectric function for GICs. Total dielectric function is the sum of dielectric functions due to impurity charge distribution, screening charge distribution and equal time correlation function between first and second electron in presence of all other electrons. This is reasonably certain because in the linear response theory total

potential is the sum of the potential due to impurity charge distribution and screening charge distribution which corresponds to Lindhard. Cooper pair energies are shown negative as a convention which represents energy release during Cooper pair formation. Problem regarding electrons with different surroundings in the calculation of $G(\mathbf{q},\omega)$ is avoided in the formalism because we either have an exciton in the normal state or a Cooper pair in BCS superconducting state. Excitation process gives a free electron pair in superconducting state or an electron-hole pair in normal state. This makes the two terms in $G(\mathbf{q},\omega)$ identical. This is essential for a better understanding of frequency dependence aspect of motion of an electron relative to the correlation hole.

4. ACKNOWLEDGEMENT

The work is supported by UGC New Delhi under UGC Fellowship in Sciences.

REFERENCES

- [1] K. S. Singwi, M. P. Tosi, R. H. Land and A Sjolander (1968) *Phys. Rev.* **170**, 2
- [2] Goran Niklasson, (1974) *Phys. Rev. B* **8**, 10
- [3] Sidharth Acharya and Raman Sharma, (2014) *Advances in Electronic and Electric Engineering*, **4**, 6
- [4] D. Pines and P. Noziers, (1966) *The Theory of Quantum Liquids*, (W. A. Benjamin, Inc. Amsterdam, New York).
- [5] Charles Kittel, (1966) *Introduction to Solid State Physics*, (John Wiley and Sons, Inc., Singapore).
- [6] S. Das Sarma and J. J. Quin, (1982) *Phys Rev. B* **25** 12.
- [7] Mahan G. D. (1964) *Many-particle Physics* (Kluwer Academic/ Plenum Publishers, New York).
- [8] Xue-Feng Wang and Tapash Chakraborty, (2007) *Phys. Rev. B* **75** 041404(R).
- [9] Jae-Huyn Choi, Hu-Jong Lee and Yong-Joo Doh (2010) *Journal of The Korean Physical Society*, 57 1
- [10] R. W. Shaw, (1970) *J. Phys. C*, **3**, 1140.